SEBHA UNIVERSITY JOURNAL OF PURE & APPLIED SCIENCES VOL.25 NO. 1 2026
DOI: 10.51984/MAZSQ207

مجلة جامعة سبها للعلوم البحتة والتطبيقية
Sebha University Journal of Pure & Applied Sciences

Journal homepage: www.sebhau.edu.ly/journal/jopas

Water Softening Performance of Crystalline α-Zirconium Phosphate

Ragiab Issa[a], Ruwayda Ghoulah[b]

[a]Chemistry Department, Faculty of Education, University of Tripoli, Tripoli, Libya.
[b]Libyan Academy for Higher Studies, Janzour, Libya.

Keywords:
Alkalinity.
Adsorption.
α-Zirconium Phosphate.
Hardness.
Isotherm.

ABSTRACT

This research focuses on drinking water softening and treatment using a simple and novel approach based on an easily prepared inorganic ion exchange material (α-zirconium phosphate). To the best of our knowledge, this is the first study to investigate the use of α-zirconium phosphate for the removal of hardness and alkalinity from water, although it has previously been applied for heavy metal removal. The study showed that percentage hardness removal decreased, while exchange capacity increased as the initial ion concentration increased. With adsorbent doses ranging from 10 to 60 g/L, percentage removal increased for both hardness and alkalinity. The contact time study showed no significant effect on percentage removal, while exchange capacity was approximately 3.3 times higher for hardness than for alkalinity. The Langmuir isotherm model showed a good fit for both hardness and alkalinity (R^2 = 0.9966 and 0.9950, respectively). The Freundlich isotherm model indicated physisorption behaviour, with n_F values of 3.08 for hardness and 20.29 for alkalinity. The Temkin isotherm model also showed a good fit with the experimental data (R^2 = 0.9259 for hardness and 0.9694 for alkalinity). The heat of adsorption (B) was found to be 9 kJ/mol for hardness, indicating physisorption, and 444 kJ/mol for alkalinity, suggesting chemisorption. Pseudo-first-order and pseudo-second-order kinetic models were applied and showed good agreement with the experimental data (R^2 = 0.9635 and 0.9999 for hardness, and 0.9195 and 0.9066 for alkalinity, respectively).

قدرة تيسير المياه باستخدام α -فوسفات الزركونيوم البلوري

رجب عيسى[a*] ورويدة غولة[b]

[a]قسم الكيمياء، كلية التربية طرابلس، جامعة طرابلس، طرابلس، ليبيا.
[b]الأكاديمية الليبية للدراسات العليا، جنزور، ليبيا.

الكلمات المفتاحية:
القاعدية.
إدمصاص.
ألفا- فوسفات الزركونيوم.
العسرة.
أيزوثيرم.

الملخص

يتناول هذا البحث موضوع تيسير ومعالجة مياه الشرب بطريقة بسيطة وجديدة تعتمد على استخدام مادة تبادل أيوني غير عضوية سهل التحضير (ألفا-فوسفات الزركونيوم). على حد علمنا، هذه هي المرة الأولى التي يتم فيها استخدام فوسفات الزركونيوم لإزالة العسرة و/أو القاعدية من الماء، إلا أنه تم استخدامه لإزالة بعض المعادن الثقيلة. وأظهر البحث أن نسبة إزالة العسرة آخذت في التناقص، في حين زادت السعة التبادلية مع زيادة تركيز الأيونات الأولية. من خلال تطبيق كتلة المادة المازة من 10 إلى 60 غم/لتر، تم زيادة نسبة إزالة الادمصاص لكل من العسرة والقلوية. أظهرت تجربة زمن التلامس عدم وجود تأثير كبير على نسبة الإزالة، في حين كانت قدرة التبادل أعلى بحوالي 3.3 مرة للعسرة من قدرة القاعدية. تم تطبيق نموذج لانجمويير المتساوي الحرارة وأظهر ملاءمة جيدة لكل من العسرة والقاعدية R^2= 0.9966 و R2= 0.9950 على التوالي. أظهر نموذج تساوي درجة حرارة فروندليش امتزازًا فيزيائيًا وفقًا لعامل عدم التجانس nF الذي كان 3.08 للعسرة و20.29 للقاعدية. يُظهر نموذج تيمكين متساوي الحرارة توافقًا جيدًا مع البيانات التجريبية، حيث كانت

*Corresponding author.
E-mail addresses: Ra.issa@uot.edu.ly, (R. Ghoulah) rwydhghwih0@gmail.com.
Article History : Received 10 February 26 - Received in revised form 05 May 26 - Accepted 21 May 26

R^2=0.9259للعسرة و0.9694 للقاعدية. وُجِد أن حرارة الادمصاص، B، تبلغ 9 كيلوجول/مول للعسرة، مما يؤكد الادمصاص الفيزيائي، و444 كيلوجول/مول للقلوية، مما يشير إلى عملية الامتزاز الكيميائي. تم تطبيق الرتبة الأولى الكاذب والدرجة الثانية ووجد أنها تتناسب بشكل جيد مع البيانات التجريبية R^2 = 0.9635 و0.9999 للعسرة و0.9195 و0.9066 للقاعدية للدرجتين الأولى والثانية على التوالي.

1. Introduction

Water hardness is a common problem worldwide that affects the quality and usability of many water sources. The main contributors to water hardness are dissolved calcium and magnesium ions, either in the form of bicarbonates, which is called temporary hardness, or in the form of sulfates, which is called permanent hardness [1]. High levels of hardness can cause serious effects, including scale buildup in appliances and pipes, reduced soap and detergent efficiency, and metal corrosion over time.

According to the World Health Organization (WHO), water with hardness less than 75 mg L^{-1} is considered soft; 75–150 mg L^{-1} is moderately hard; 150–300 mg L^{-1} is hard; and above 300 mg L^{-1} is very hard.

In addition to hardness, alkalinity (carbonate, bicarbonate, and hydroxide ions) is an important parameter. Alkalinity can cause foaming and carryover of solid particles in steam, which can lead to weakening of boiler steel. Bicarbonate and carbonate ions generate CO_2 in steam, which contributes to corrosion [2].

Various water treatment methods have been proposed, including ion exchange resins, boiling, reverse osmosis, and inorganic ion exchangers. The most widely reported inorganic ion exchange materials are based on tetravalent metals such as zirconium, hafnium, titanium, and germanium. In the 1960s, crystalline α-zirconium phosphate (α-ZrP) was first reported by Clearfield et al. [3], with the formula $Zr(HPO_4)_2 \cdot H_2O$. The crystalline phase was synthesized by refluxing amorphous zirconium phosphate with concentrated orthophosphoric acid [4].

Zirconium phosphate (ZrP) is widely used as an adsorbent for removing heavy metals, dyes, and other contaminants due to its phosphate groups, which enable ion exchange with contaminants [5]. However, it is limited in fixed-bed or flow-through systems due to high pressure drop and poor mechanical strength resulting from its fine submicrometric particle size [6].

Layered zirconium phosphate (ZrP) has been combined with a cation exchanger (D-001) and investigated for the adsorption of Pb^{2+}, Zn^{2+}, and Cd^{2+}. The composite showed high selectivity for lead compared to zinc and cadmium [7]. During the past five decades, several crystalline phases of zirconium phosphate have been synthesised, including β-$Zr(HPO_4)(H_2PO_4)$, γ-$Zr(PO_4)(H_2PO_4) \cdot H_2O$ [8], and θ-$Zr(HPO_4) \cdot 6H_2O$ [9], and other phases, and applied for heavy metal removal under different conditions.

The α-type zirconium phosphate has a layered structure with an interlayer spacing of 7.56 Å, which facilitates intercalation as well as surface adsorption [10,11]. This study investigates α-zirconium phosphate (α-ZrP) for the removal of hardness and alkalinity from groundwater. Isotherm and kinetic models were applied to study water hardness and alkalinity removal.

2. Materials and Methods

2.1. Preparation of α -ZrP

A modified approach was used to synthesize the ion exchanger α-zirconium phosphate according to Horsley and Nowell, 1973 [11]. One litre of deionized water was used to dissolve 100 g of oxalic acid, $C_2H_2O_4$ (from BDH). Ten grams of zirconyl oxo-chloride, $ZrOCl_2.8H_2O$ (from MERCK), were added to the oxalic acid solution after being dissolved in a suitable volume of deionized water. 20 mL of orthophosphoric acid, H_3PO_4, 88% (from Analytical Rasayan), was added after the zirconyl chloride had completely dissolved. The mixture was heated to 80°C after being diluted to 1.5 litres with water and stirred. After seven hours, the liquid was chilled and repeatedly decanted until the pH was greater than three in order to remove any remaining chloride ions. The white microcrystal precipitate was filtered out and stored for characterization and application tests after the pH was adjusted to be >3. It was determined that the yield percentage of generated α-ZrP was approximately 16%.

2.2. Preparation and Analysis of Water Samples

From a groundwater well 30 m deep in Sabratha City, Libya. After keeping water flow for about 20minutes, some physical properties were immediately measured (i.e., pH = 6.8, temperature = 17.5 °C), then 20 liters of water were collected, chemically analyzed for hardness and alkalinity, and kept in a dark container at about 25 °C for proceeding all other experiments. Hardness was determined by the EDTA titration method, and alkalinity was measured by the acid titration method [12]. For the initial ion concentration, the sample has been diluted in a series of 10, 30, 50, 70, and 90% with deionized water. The average of 3 replicates ±SD and ±RSD of the chemical analysis of total hardness and alkalinity for all these fractions is given in Tables 1 and 2, respectively.

These samples were analyzed for hardness and alkalinity; the same samples were prepared, and 0.1 g of ion exchanger was added to each one. Samples were kept statically for 24 hours and then filtered and analyzed for hardness and alkalinity. For the experiment of adsorbent amount, a series of 0.1, 0.2, 0.3, 0.4, 0.5, and 0.6 g of the ion exchanger was transferred to six 100 mL flasks and filled to the mark with the original water sample. These samples were also analyzed for hardness and alkalinity. Contact time was investigated by adding 0.1 g of the ion exchanger to 7 flasks and filling them with the original water sample. The flasks containing the exchanger were kept for 30, 60, 90, 120, 240, 280, and 300 minutes. After every significant period of time, the samples were filtered, and the concentration of hardness and alkalinity was determined. Every determination was carried out three times according to an official method of water analysis [13].

Table 1: Total harness chemical analysis of water fractions

Dilution%	Total hardness		
	Average	SD	RSD (%)
10	293	± 11.54	± 3.94
30	860	± 20.00	± 2.33
50	1380	± 20.00	± 1.49
70	1952	± 11.55	± 0.59
90	2540	± 34.64	± 1.36
100	2966	± 30.55	± 1.03

Table 2: Alkalinity chemical analysis of water fractions

Dilution%	Alkalinity		
	Average	SD	RSD (%)
10	25	±1.88	±7.53
30	50	±1.88	±3.77
50	76	±1.88	±2.47
70	104	±5.63	±5.42
90	134	±4.96	±3.70
100	143	±3.25	±2.27

Percent removed was calculated according to equation 1, and the experimental exchange capacity was calculated using equation 2; both tasks were plotted together for the different parameters. Finally, isotherm models (i.e., Langmuir, Freundlich, and Temkin) and the kinetic models of pseudo-first order and pseudo-second order were also investigated.

$$\% \, removed = \frac{C_i - C_e}{C_i} \times 100 \qquad (1)$$

$$q_e = (C_i - C_e) \times \frac{V}{m} \qquad (2)$$

Where, C_i and C_e are the initial and equilibrium solution concentrations, q_e is the experimental exchange capacity, V is the solution volume (L), and m is the adsorbent mass (g).

3. Results and Discussion

3.1. X-ray Diffraction (XRD)

Figure 1 displays the XRD patterns of α-ZrP. The characteristic diffraction peaks of d (002), d (110), and d (112) are represented by the three primary strong diffraction peaks at 2□□(d-spacing), which are equivalent to 11.84° (7.48Å), 19.86° (4.47Å), and 25.03° (3.36Å). Additionally, the x-ray pattern shows distinct peaks at 33.90° and 48.57°, which correspond to the d-spacing of 2.64 Å and 1.87 Å, respectively. These numbers are extremely similar to those found earlier [14]. As a result, the degree of crystallinity was determined to be between 21 and 26 nm.

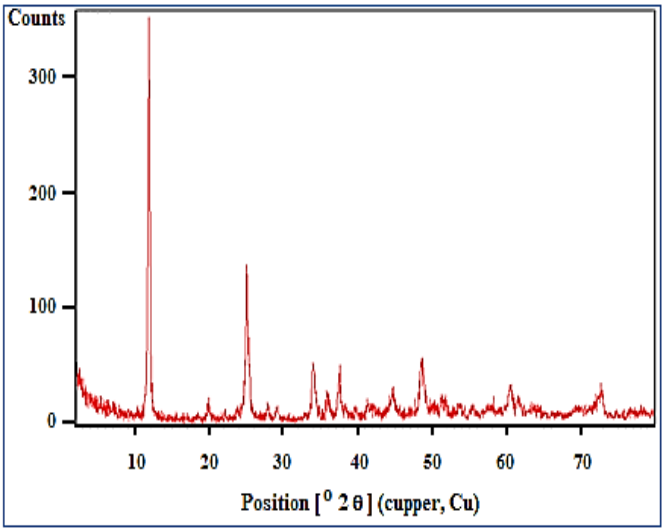

Figure 1: X-Ray diffraction pattern of α-zirconium phosphate

3.2. Thermogravimetric Analysis (TGA)

The thermogram of α-zirconium phosphate is displayed in Figure 2, which clearly exhibits two plateaus. The first one occurs at roughly 309 °C, when 4% of the first-level interlayer of coupled water is lost, resulting in $Zr(PO_4)_2$. Figure 2 depicts an incomprehensible peak rising between ambient and 100 °C, followed by a modest plateau at less than 200 °C.

The hydrolysis of $Zr(HPO_4)_2.nH_2O$ to a dominant form, zirconium pyrophosphate ZrP_2O_7, was indicated by the loss of 6.4% at around 596 °C [14], [15]. As a result, $Zr(HPO_4)_2.0.22H_2O$ is thought to be the structure of the generated chemical. However, the high breakdown temperature suggests that α-ZrP is thermally stable and able to preserve its layered structure.

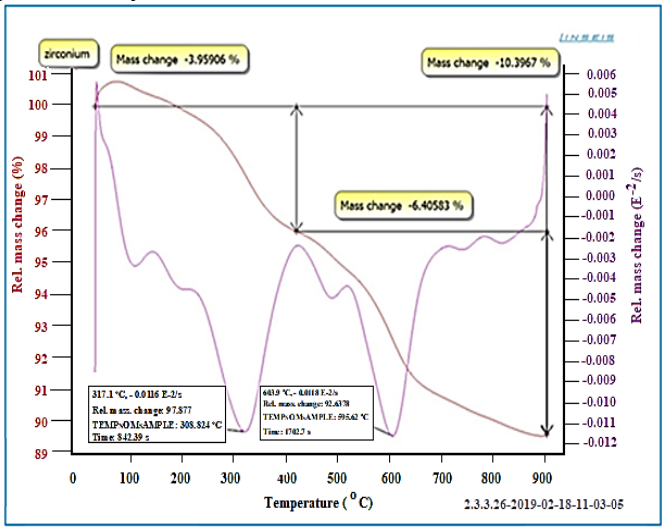

Figure 2: Thermogravimetric analysis of α-zirconium phosphat3.3. Effect of Initial Ion Concentration

Figure 3 shows the effect of the initial hardness concentration as adsorbed on α-ZrP; the % removed decreased (from 47 to 30%) with increasing hardness along the dilution factor from 10 to 90% from the original water sample. This could be due to reducing the active sites on the adsorbent surface as the concentration of the adsorbate increases. On the contrary, the experimental exchange capacity (q_e) increases from 130 to about 800 mg/g. This behavior is true for many other applications of adsorbing heavy metals on α-ZrP [6].

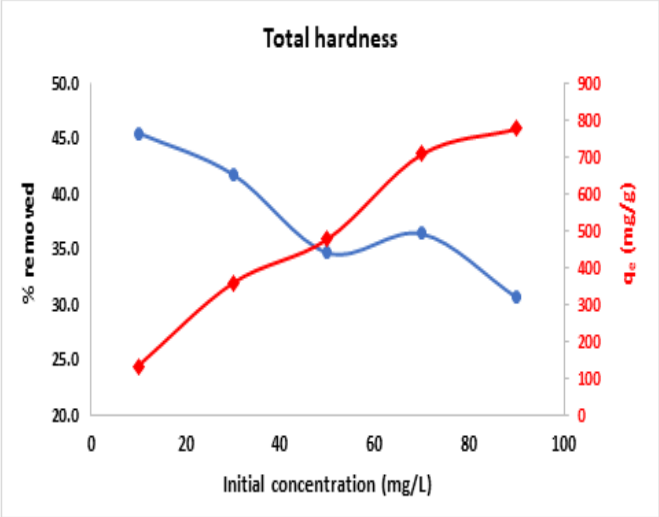

Figure 3: Effect of initial ion concentration on the adsorption hardness

3.4. Effect of Adsorbent Amount

As the adsorbent mass increases, the % removed increases from 1 to about 17% for total hardness and from 22 to about 95% for alkalinity. For hardness, it shows a sharp increase from 0.3 g to 0.4 g, while it was gradually linear, lower than 0.3 g, and higher than 0.4 g for the adsorbent. For alkalinity, however, it shows a bit sharp; at less than 0.2 g of the adsorbent, it gives a gradual increase from 0.2 to 0.6 g of the adsorbent (Figure 4). The Figure also shows an increase in the exchange capacity up to 0.4 g of the absorbent, where it was increased from 50 to 200 mg/g. After 0.4 g, it decreased to 160 mg/g. For alkalinity, there was almost no effect at less than 0.3 g, and it decreased from 70 to 42 mg/g when the adsorbent mass increased from 0.3 to 0.6 g.

3.5. Effect of Contact Time

Figure 5 shows small positive effects of contact time on the % removed and the exchange capacity for both hardness and alkalinity. The % removal was increased by 25% for hardness and 25% for alkalinity, showing about 6 time increasing for alkalinity than for hardness. The adsorption capacity for hardness was more than 3.4 times higher than that for alkalinity, 450 to 130 mg. g^{-1}.

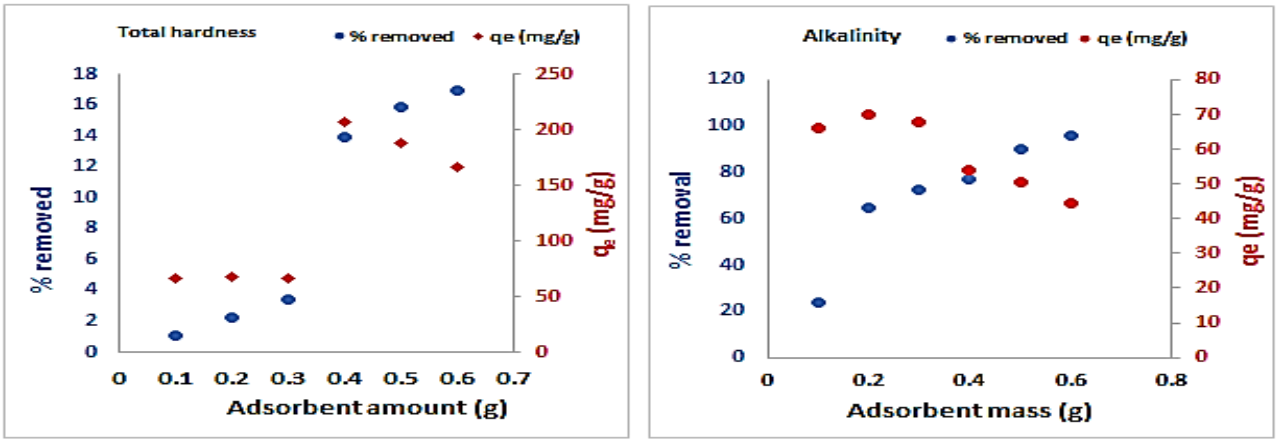

Figure 4: Effect of adsorbent amount on the adsorption hardness and alkalinity

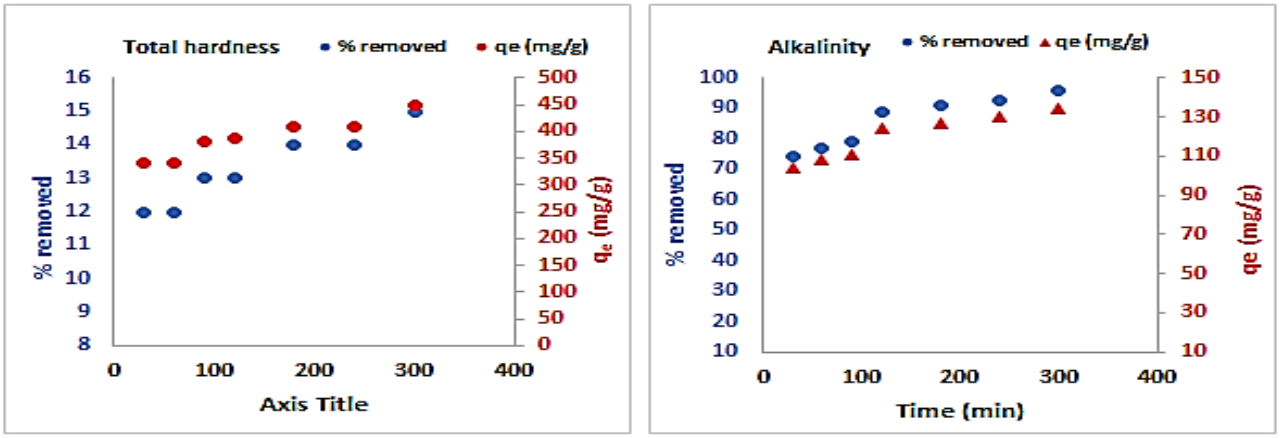

Figure 5: Effect of contact time on the adsorption hardness and alkalinity

4. Isotherm Models

Several mathematical models, such as the Langmuir model, the Freundlich model, and the Temkin model, were used to investigate the adsorption of hardness and alkalinity onto α-ZrP. The interaction between the adsorbent and the adsorbate must be understood in order to comprehend the mechanism of the adsorption process. This makes it easier to fit the adsorption data to various model-controlled adsorption isotherms.

4.1. Langmuir Model

The Langmuir sorption isotherm is applied to equilibrium sorption under the assumption of monolayer sorption onto a surface with a finite number of identical sites. Equations 3 and 4 are the Langmuir equations, according to Langmuir 1916, [16].

$$\frac{1}{q_e} = \frac{1}{Q_m} + \frac{1}{bQ_mC_e} \qquad (3)$$

The form of this isotherm can alternatively be expressed using the separation factor (R_L), which is given as follows [17]:

$$R_L = \frac{1}{1 + K_L C_i} \qquad (4)$$

where K_L is the Langmuir constant (L/mg) associated with the sorption free energy and binding site affinity. The equilibrium capacity (mg/g) measured experimentally is denoted by $\mathbf{q_e}$. C_e is the concentration of the ions in solution at equilibrium (mg/L). Q_{max} is the maximum equilibrium capacity that can be calculated using the model (mg/g). Equations 5 and 6 are used to determine Q_m and K_L, respectively.

$$Q_{max} = \frac{1}{slope} \qquad (5)$$

$$k_L = \frac{1}{Q_{max} \times intercept} \qquad (6)$$

The Langmuir curve (Figure 6) yielded a maximum exchange capacity of 1667 mg. g^{-1} for hardness, which is higher than the experimental value of 200 mg. g^{-1} (Figure 3). For alkalinity, the Q_{max} = 6.37 mg/g, which is about 100 times less than the experimental data. The model's points have an acceptable correlation coefficient (R^2 = 0.8765 for hardness and 0.9072 for alkalinity), as seen in Figure 6, demonstrating effective hardness and alkalinity adsorption onto α-ZrP.

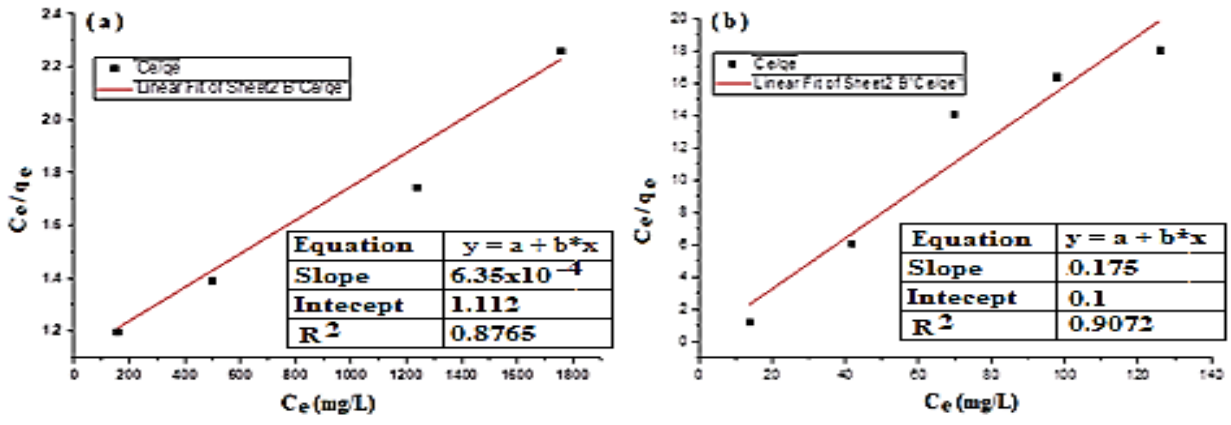

Figure 6: Langmuir isotherm model for the adsorption of total hardness (a) and alkalinity (b) α-ZrP.

Because the Langmuir isotherm equation is developed from thermodynamic principles, one important element that may be predicted is the separation factor (R_L), [18]. The separation factor is a measure of the conditions of the adsorption system based on the criteria of linearity ($R_L = 1$), appropriateness ($0< R_L<1$), unsuitability ($R_L>1$), or irreversibility ($R_L = 0$). For adsorbent concentrations of 1 mg/L, the models's R_L values were 0.385 and $4.5x10^{-3}$ for hardness and alkalinity, respectively. As can be seen, the R_L for hardness is about 86 times higher than that for alkalinity, showing the suitability of adsorption for both components onto α-ZrP. Langmuir constants (K_L) were, $5.4x10^{-4}$ and 1.57 $L.mg^{-1}$ for total hardness and alkalinity respectively, indicating that the adsorption of alkalinity is faster than that for hardness.

4.2. Freundlich Model

Another idea that has been put into view is Freundlich's adsorption mechanism. The creation of heterogeneous adsorbate layers, which may be explained empirically, is consistent with this isotherm. The Freundlich equation for heterogeneous surface energy systems is represented by equation 7, [19], [20].

$$\log(q_e) = logK_F + \frac{1}{n} logC_e \qquad (7)$$

where the plot of ln q_e versus ln C_e yields the Freundlich constants, K_F and **n**. The system's sorption capacity and sorption intensity are correlated with the parameters K_F and ***1/n***. The favorability of the adsorbent/adsorbate systems is shown by the size of the term (***1/n***), [21]. Equation 8 is used to determine K_F, and equation 9 uses ***1/n*** as the slope.

$$logK_F = intercept \qquad (8)$$

$$\frac{1}{n} = slope \qquad (9)$$

The heterogeneity factor (n_F), a parameter, can be measured using the Freundlich thermodynamic curve. The adsorption mechanism is therefore categorized as either chemisorption ($n_F < 1$), physical adsorption ($n_F > 1$), or linear ($n_F = 1$). This value can also be used to quickly ascertain whether the process follows the typical Freundlich thermodynamic curve [$(\frac{1}{n_F}) > 1$.

The modelling data obtained in Figure 7, show the Freundlich isotherms (R^2 = 0.981 and 0.956 for hardness and alkalinity, respectively). The correlation coefficient (R^2) indicates that the Langmuir model performs slightly better than the Freundlich model for the adsorption of both hardness and alkalinity onto α-ZrP. n_F is 3.08 and 20.29 for hardness and alkalinity, respectively, which indicates that the adsorption process is more favorable for alkalinity and that more solute molecules can be adsorbed as the concentration increases.

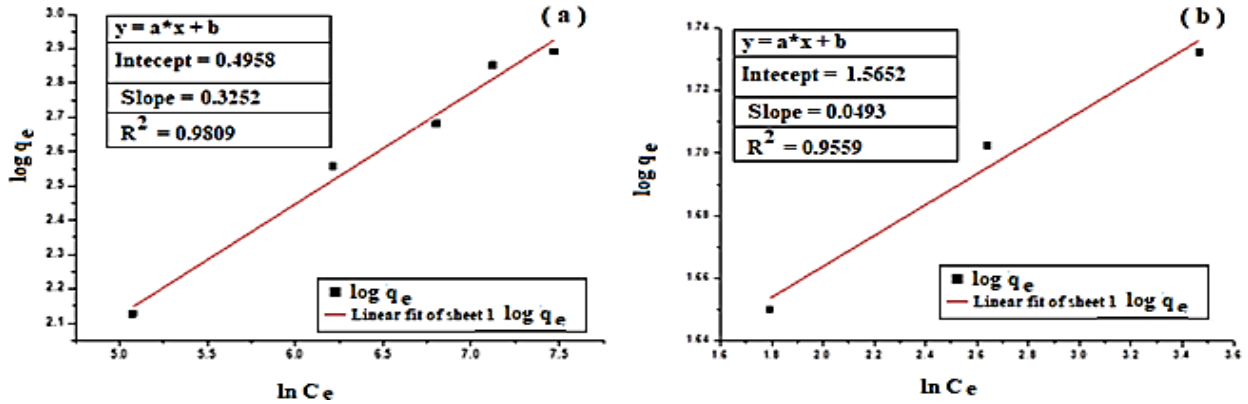

Figure 7: Freundlich isotherm model for the adsorption of total hardness (a) and alkalinity (b) α-ZrP.

4.3. Temkin Model

Adsorbent-adsorbate interactions are reflected in the Temkin equation, an adsorption isotherm model that explains how the heat of adsorption reduces linearly with surface coverage [22]. Equation 10 illustrates how it is frequently expressed in a linear form.

$$q_e = B_T \ln k_T + B_T \ln C_e \qquad (10)$$

where q_e is the amount of adsorbate at equilibrium, C_e is the equilibrium concentration, K_T is the binding constant, B_T is the constant associated with the heat of adsorption, R and T are the absolute temperature in Kelvin and the gas constant (8.314 J/mol K), respectively, and ***b*** is the Temkin constant associated with the heat of sorption (J/mg).

The Temkin constant (b_T), which is directly related to the heat of adsorption (ΔH) and shows whether the process is chemical or physical, can be calculated using equation 10. It is equal to the slope (equation 11).

$$b_T = slope \qquad (11)$$

Equation 12 was used to get the equilibrium binding constant (K_T), which represents the maximum binding energy accessible during the adsorption phase.

$$K_T = e^{(intercept/b_T)} \qquad (12)$$

The Temkin thermodynamic equation describes multiple layers and their potential interactions using a thermodynamic approach. The Temkin thermodynamic equations are based on the assumption that the maximum adsorption energy is evenly distributed and that the molecules in the covered layer lose heat of adsorption linearly. [22].

The Temkin constant can be used to approximate the thermodynamic coefficient constant b_T using the temperature T in kelvin [K] and the gas constant R = 8.314 J. $K^{-1}.mol^{-1}$.

The heat of adsorption, $B = RT/b_T$, is calculated using the expected value of b_T (Figure 8). Generally, when the value of B is less than 40 kJ/mol, the adsorption is called physical, while if the value of B is greater than this, the adsorption is called chemical adsorption.

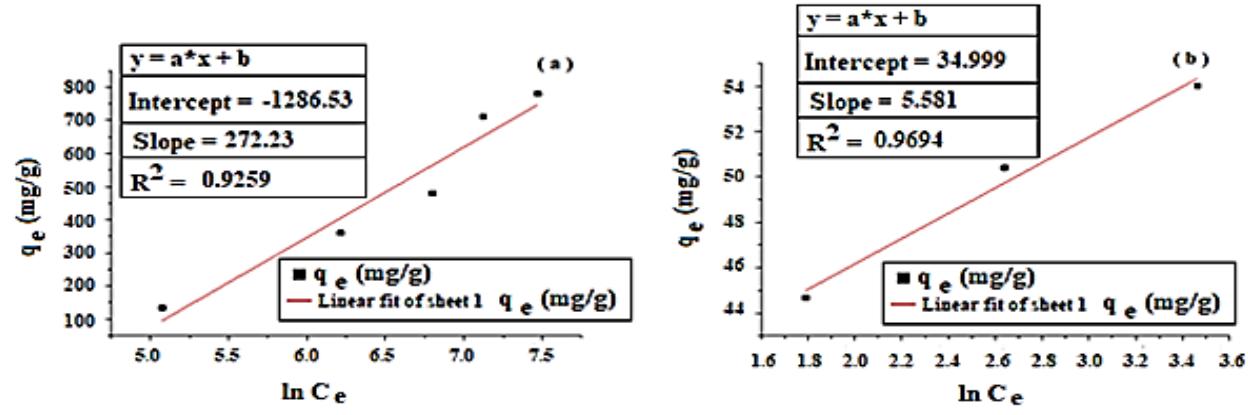

Figure 8: Temkin isotherm model for the adsorption of total hardness (a) and alkalinity (b) on α-ZrP.

In our case, B = 9 kJ/mol for hardness (physisorption) and 444 kJ/mol for alkalinity (chemosorption); therefore, the adsorption is considered chemical in the case of alkalinity while it is physical in the case of hardness. The Temkin model exhibits a good correlation coefficient, $R^2 = 0.9251$ for hardness and 0.9694 for alkalinity. It is considered the best compared to the Langmuir model and the Freundlich model.

5. Kinetic Experiment Model

Using the data from the effect of time experiment, two models for kinetic adsorption have been plotted.

5.1. Pseudo First Order

A pseudo-first-order model is expressed by the curve for ln(qe-qt) against time (**t**) in Figure 9. The model fits the experimental data well, as indicated by the correlation coefficient R^2=0.9835 for hardness and 0.9198 for alkalinity. K_1=-slope was found to be $3.88 \times 10^{-4} min^{-1}$ for hardness and $1.65 \times 10^{-2}\ min^{-1}$ for alkalinity, and $\mathbf{q_e}$, which was determined using the formula $q_e = e^{intercept}$, was 2618 mg.g^{-1} for hardness and 72.2 mg. g^{-1} for alkalinity, indicating that the model was more reliable for hardness than alkalinity.

5.2. Pseudo-Second Order

A curve for **t/qt** against **t/q_e** that corresponds to the pseudo-second model is shown in Figure 10. According to the calculations, the correlation coefficient $R^2 = 0.9999$ for hardness and 0.9066 in the case of alkalinity. $q_e = 3.61 \times 10^{-4} mg.g^{-1}$ for hardness and 7.25×10^{-3} mg. g^{-1} for alkalinity, respectively. The adsorption constant $K_2 = 1.34 \times 10^{-11} min^{-1}$ for hardness and $K_2 = 5.35\ min^{-1}$ For alkalinity, however, it was a slow adsorption process, R^2 is demonstrating a perfect fit between the model and the experimental data in the case of hardness and weak compatibility for alkalinity. The equations applied to these calculations are:

$\frac{t}{q_e} = \frac{1}{K_2 q_e^2} + \frac{1}{q_e}$, $intercept = \frac{1}{K_2 q_e^2}$, $K_2 = \frac{1}{intercept}$, and $q_e = \frac{1}{slope}$.

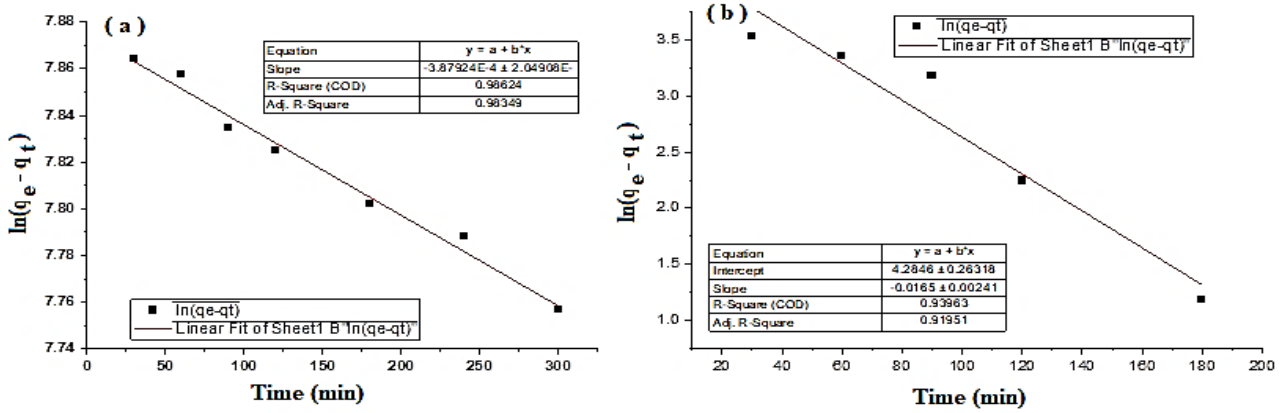

Figure 9: Pseudo first order for the adsorption of total hardness (a) and alkalinity (b) on α -ZrP

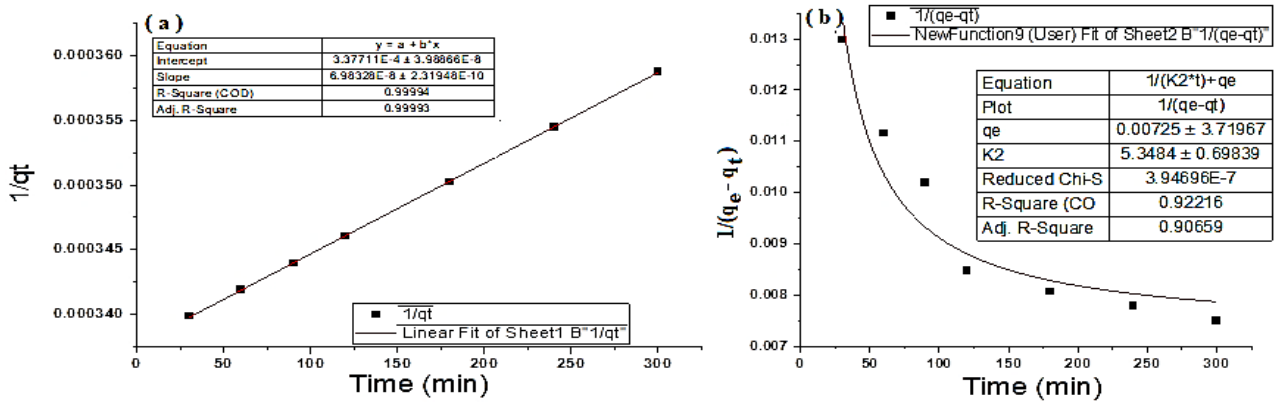

Figure 10: Pseudo-second order for the adsorption of total hardness (a) and alkalinity (b) on α-ZrP.

6. Conclusion

The conclusion of this study confirmed that α-ZrP can be readily prepared in the laboratory and applied for reducing hardness and alkalinity in very hard water, with initial hardness of 2960 mg L^{-1} and alkalinity of 140 mg L^{-1}, both expressed as $CaCO_3$. The study showed that percentage removal increased as the adsorbent mass decreased and decreased with increasing initial ion concentration. However, percentage removal reached only 17% for hardness at an adsorbent dose of 60 g L^{-1}, while it exceeded 90% for alkalinity.

The experimental data gave an acceptable fit with the Langmuir, Freundlich, and Temkin isotherm models. It was also consistent with both pseudo-first-order and pseudo-second-order kinetic models. The Freundlich and Temkin isotherm models indicated physisorption for hardness, while the Temkin model indicated chemisorption for alkalinity.

The authors recommend applying this ion exchanger in less hard water systems and developing composite materials to improve adsorption performance.

7. Acknowledgments

The authors would like to express their gratitude to Sabratha University's Faculty of Engineering for providing the resources needed for this study's experimental work.

8. References

[1] Joshi A., Hande S., Chorghade V., Devale P., and Gargade P., Determination and Removal of Hardness of Water, International Journal of Novel Research and Development, Volume 8, Issue 10 October 2023 pp 224-229, ISSN: 2456-4184.

[2] Cheremisinoff, N. P., Handbook of water and wastewater treatment technology, 2002 by Butterworth-Heinemann, ISBN: 0-7506-7498-9.

[3] Clearfield A, Oskarsson A, Oskarsson C. On the mechanism of ion exchange in crystalline zirconium phosphates. VI. The effect of crystallinity of the exchanger on Na^+/H^+ exchange. Ion Exch Membr. 1972 Dec;1(2):91-107. PMID: 4680660.

[4] Cheng Y. Chuah G. K. The synthesis and applications of α-zirconium phosphate, Chin. Chem. Lett. (2019), https://doi.org/10.1016/j.cclet.2019.04.063.

[5] Pica M. Treatment of Wastewaters with Zirconium Phosphate Based Materials: A Review on Efficient Systems for the Removal of Heavy Metal and Dye Water Pollutants. Molecules. 2021 Apr 20;26(8):2392. doi: 10.3390/molecules26082392. PMID: 33924121; PMCID: PMC8074336.

[6] Pan BC, Zhang QR, Zhang WM, Pan BJ, Du W, Lv L, Zhang QJ, Xu ZW, Zhang QX. Highly effective removal of heavy metals by polymer-based zirconium phosphate: a case study of lead ion. J Colloid Interface Sci. 2007 Jun 1;310(1):99-105. doi: 10.1016/j.jcis.2007.01.064. Epub 2007 Mar 2. PMID: 17336317.

[7] Zhang QR, Du W, Pan BC, Pan BJ, Zhang WM, Zhang QJ, Xu ZW, Zhang QX. A comparative study on Pb^{2+}, Zn^{2+}, and Cd^{2+} sorption onto zirconium phosphate supported by a cation exchanger. J Hazard Mater. 2008 Apr 1;152(2):469-75. doi: 10.1016/j.jhazmat.2007.07.012. Epub 2007 Jul 10. PMID: 17706343.

[8] Cheng, Yu; Dong (Tony) Wang, Xiao; Jaenicke, Stephan; Chuah, Gaik-Khuan. (2018). *Mechanochemistry-Based Synthesis of Highly Crystalline γ-Zirconium Phosphate for Selective Ion Exchange. Inorganic Chemistry, (), acs.inorgchem.7b03202*– .doi:10.1021/acs.inorgchem.7b03202.

[9] Krog Andersen K., A. M.; Norby A. M., P.; Hanson, J. C.; Vogt, TPreparation and Characterization of a New 3-Dimensional Zirconium Hydrogen Phosphate, τ-Zr(HPO4)2. Determination of the Complete Crystal Structure Combining Synchrotron X-Ray Single-Crystal Diffraction and Neutron Powder Diffraction. Inorg. Chem. 1998, 37, 876−881.

[10] Qureshi M. and Varshney K. G., Inorganic ion exchangers in chemical analysis, CRC Press, Inc., 2000 Corporate Blvd., N.W., Boca Raton, Florida 33431.

[11] Horsley S. E., and Nowell D. V. (1973) The Preparation and Characterisation of Crystalline α-Zirconium Phosphate, *J. appl. Chem. Biotechnol.*,23,215-224.

[12] APHA, (American Public Health Association) (2017). Standard methods for the examination of waters and wastewaters. APHAAWWA- WEF, Washington, DC.

[13] Brown E., Skougstad M. W., and Fishman M. J., Methods for collection and analysis of water samples for dissolved minerals and gases, (1970) United States Government Printing Office, Washington.

[14] Han, L., Chen, Q., Chen, H., Yu, S., Xiao, L., & Ye, Z. (2018). Synthesis and Performance of Functionalized α-Zirconium Phosphate Modified with Octadecyl Isocyanate. Journal of Nanomaterials, 2018, 1–9. doi:10.1155/2018/5873871.

[15] Shuai M., Mejia A. F., Chang YW., and Cheng Z. (2013) Hydrothermal synthesis of layered α-zirconium phosphate disks: control of aspect ratio and polydispersity for nano-architecture, CrystEngComm, 2013, 15, 1970–1977, DOI: 10.1039/c2ce26402a.

[16] Langmuir I., (1916). The constitution and fundamental properties of solids and liquids. Part I. Solids, Journal of the American Chemical Society, vol. 38, no. 11, pp. 2221–2295.

[17] Cheruiyota G. K., Wanyonyia W. C., Joycea K. J., and Maina E. N. (2019) Adsorption of Toxic Crystal Violet Dye Using Coffee Husks: Equilibrium, Kinetics and Thermodynamics Study, Scientific African, https://doi.org/10.1016/j.sciaf.2019.e00116.

[18] Weber, T. W., and Chakravorti, R. K., (1974) Pore and solid diffusion models for fixed-bed adsorbers, AICHE Journal, vol. 20, no. 2, pp. 228–238.

[19] Alkherraz A. M., Elsherif K. M., Madiry A. H. (2025) Kinetic Isotherm and Thermodynamic Modelling of Methylene Blue Adsorption Using Green Tea-Based Biosorbents, The Libyan Journal of Science, University of Tripoli Vol. 28, No. 01.

[20] Pathania D., Sharma S., Singh P. (2017) Removal of methylene blue by adsorption onto activated carbon developed from Ficus carica bast, Arabian Journal of Chemistry 10, S1445–S1451.

[21] Malik P. K., (2003) Use of activated carbons prepared from sawdust and rice-husk for adsorption of acid dyes: a case study of Acid Yellow 36, Dyes and Pigments 56, 239–249.

[22] Sulthana R., Taqui S. N., Syed U. T., Khan T. M.Y., Abdul Khadar S. D., Mokashi I., Shahapurkar K., Kalam M. A., Murthy H. C. A., and Syed A. A. (2022) Adsorption of Crystal Violet Dye from Aqueous Solution using Industrial Pepper Seed Spent: Equilibrium, Thermodynamic, and Kinetic Studies, Hindawi, Adsorption Science & Technology, Volume 2022, Article ID 9009214, 20 pages https://doi.org/10.1155/2022/9009214.